Available online at www.sciencedirect.com
ScienceDirect
Journal of Crystal Growth 310 (2008) 2365–2369
JOURNAL OF CRYSTAL GROWTH
www.elsevier.com/locate/jcrysgro

Growth and characterization of GaInAsP/InP-based Geiger-mode avalanche photodiodes ☆

D.C. Chapman*, C.J. Vineis, D.C. Oakley, A. Napoleone, G.M. Smith, E.K. Duerr, K.E. Jensen, J.P. Donnelly, K.A. McIntosh, S. Verghese

Lincoln Laboratory, Massachusetts Institute of Technology, 244 Wood St., Lexington, MA 02420-9108, USA

Available online 19 November 2007

Abstract

Geiger-mode avalanche photodiodes (GM-APDs) grown by organometallic vapor phase epitaxy are of interest for several low-light-level applications, including laser radars and single-photon-counting optical communications. Materials systems based on GaInAsP lattice matched to InP are critical to the performance of GM-APDs at both 1.06- and 1.55-μm wavelengths. Growth temperature, growth rate, and V/III ratio were investigated to determine the effect each had on important device parameters, dark count rate and after-pulsing. Improvements of growth conditions led to a 44% reduction in dark count rate (DCR), but after-pulsing behavior, and thus dead time of GM-APDs was unaffected. The improvement of growth conditions has led to devices with DCRs at 300 K of 8×10^9 Hz/cm^2 with dead times still at approximately 1 μs.

PACS: 81.05.Ea; 81.15.Gh

Keywords: A3. Organometallic vapor phase epitaxy; B2. Semiconducting III–V materials; B3. Infrared devices

1. Introduction

Avalanche photodiodes (APDs) operated in Geiger-mode (GM) are sensitive detectors used in optical applications that require the ability to detect the arrival of single photons [1]. GM-APDs based on materials systems lattice matched to InP span the wavelengths of InP (922 nm) to GaInAs (1654 nm). Materials and fabrication improvements have yielded devices which can detect the arrival of photons with <0.5 ns timing and photon detection efficiencies (PDEs) of approximately 50%. At MIT Lincoln Laboratory, efforts have focused on GaInAsP/InP-based 1.06-μm and GaInAs/InP 1.55-μm sensitive APDs for short-wave infrared (SWIR) wavelength applications.

Two applications driving the development of GM-APDs are laser Radar (LADAR) and free space laser communication. Both applications require arrays of APDs bump-bonded to CMOS read-out integrated circuits that can time stamp the arrival of the photons. Overall system performance is governed by the dark count rate (DCR) and the PDE. A third parameter, the dead time (T_r), determines the time the APD must be held below its breakdown voltage after firing before it can be rearmed (biased beyond breakdown) without causing an after-pulse dark count [2,3]. The dead time is especially important for laser communications systems that are similar to the recently canceled Mars Laser Communications Demonstration [4]. The system demands for array performance have pushed the development of the materials systems in order to reduce the DCR to less than 1×10^{10} Hz/cm^2, decrease the dead time to less than 1 μs, and increase the PDE up to 50%.

In GM operation, the APD is biased a few volts beyond the breakdown voltage which puts the materials under

☆This work was sponsored by the National Aeronautics and Space Administration under United States Air Force contract number FA8721-05-C-0002. Opinions, interpretations, conclusions and recommendations are those of the authors and are not necessarily endorsed by the United States Government.

*Corresponding author. Tel.: +1 781 981 3658; fax: +1 781 981 0122.
E-mail address: chapman@ll.mit.edu (D.C. Chapman).

0022-0248/$ - see front matter © 2007 Elsevier B.V. All rights reserved.
doi:10.1016/j.jcrysgro.2007.11.043

extremely stressful conditions. This makes material quality paramount as impurities can have detrimental effects on device performance. In this metastable state, a photon has a high probability of creating an electron–hole pair that can cause an avalanche event. In addition to photons, avalanche events can be caused by non-photon related processes. Dark counts are avalanche events caused by thermally generated carriers or tunneling events that are indistinguishable from events caused by a photon-generated carrier [5]. These events are often assisted by traps that are in the band gap of the material caused by native defects in the crystal. In addition to dark counts, after-pulsing is a related phenomenon that can cause an avalanche event. After-pulsing is caused by a small fraction of carriers that get trapped by defects during an avalanche event [2,6]. After the avalanche event is over, the trapped carriers depopulate via a field-assisted thermal process. If the APD is biased beyond breakdown before the traps depopulate, an avalanche event can occur, causing a dark count [3]. In order to minimize DCR and after-pulsing it is necessary to identify and then mitigate creation of native defects in the materials.

This paper describes improvements in growth conditions and characterization of InP-based materials to be fabricated into single-photon sensitive detectors and relates changes in OMVPE growth conditions to device performance. By understanding the defect equilibria, we try and identify defects responsible for dark counts and after-pulsing, and improve growth conditions to minimize defect formation and improve dark count and after-pulsing performance. It is found that DCR is improved by changes to OMVPE growth conditions, but after-pulsing remains unaffected.

2. Experimental procedure

GaInAs(P)/InP-based GM-APDs were grown on nominally (1 0 0) oriented InP substrates by OMVPE using a low pressure close-coupled showerhead reactor. Devices have been grown on n^+ InP substrates as well as p^+, n^-, and p^- InP substrates. Trimethylindium, trimethylgallium, arsine, and phosphine were used as precursors. Disilane and diethylzinc were used as dopant sources. GaInAsP lattice matched to InP is used for 1.06-μm APDs and GaInAs lattice matched to InP is used for 1.55-μm absorber material in the GM-APDs.

Fig. 1 shows the standard design for a mesa-isolated GM-APD. The structure has been optimized by considering design tradeoffs leading to low DCR and high PDE. This includes appropriately tailoring the thicknesses of the avalanche layer, the absorber layer, and the thickness and doping level of the field stop layer [7]. Current devices have a 1.4 μm thick avalanche and a 1.5 μm thick absorber. The field stop doping and thickness are adjusted to give the appropriate breakdown voltage and electric field profiles for the required operating conditions. The design also includes graded GaInAsP layers to address thermal barrier

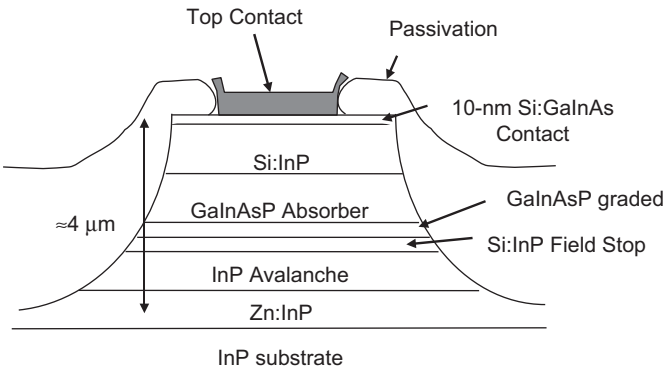

Fig. 1. Standard design for mesa-isolated InP-based GM-APDs. The design includes graded GaInAsP layers and step doping of the Zn:InP layer.

heights that may inhibit minority carrier flow from the absorber to the avalanche. This is more important for 1.55-μm devices and when GM-APDs are operated at lower temperatures. Additionally, Zn doping concentration in the 2.0 μm p-contact layer was modified such that the last 0.5 μm is doped at $8 \times 10^{17}\,cm^{-3}$ compared to $1.6 \times 10^{18}\,cm^{-3}$ to limit Zn diffusion into the multiplier (avalanche) region.

The majority of experiments focused on growth conditions for the InP avalanche region. This was accomplished by replacing the GaInAsP or GaInAs absorber layer with InP to make a "dummy" GM-APD consisting of only InP in order to separate the contributions of the absorber from that of the avalanche layer on device performance. Changes in growth conditions were only done for the InP avalanche layer. Growth conditions were fixed for all other layers. Thus, the growth temperature was varied from 600 to 650 °C, the V/III ratio was varied from 55 to 330, and the growth rate was varied between 1.5 and 10.3 Å/s for the InP avalanche layer. Once growth conditions for the "dummy" GM-APD were tested, 1.06- or 1.55-μm GM-APDs were grown, fabricated, and tested.

After OMVPE growth, materials were characterized using photoluminescence (PL) and X-ray diffraction (XRD) to ensure wafer uniformity and lattice matching. Samples were then fabricated using standard procedures into mesa-isolated APDs. Measurements for DCR and after-pulsing were done on GM-APDs of various diameters in nitrogen purged, temperature controlled chambers. The after-pulsing measurement techniques are described in detail in Ref. [2]. Secondary ion mass spectroscopy (SIMS) and deep level transient spectroscopy (DLTS) were performed to determine impurities and defect levels in the materials.

3. Results and discussion

To determine material quality, samples were sent for SIMS and DLTS measurements. SIMS measurements performed on samples grown at 625 °C, V/III ratio of 110, and growth rate of 7.9 Å/s showed doping profiles for

both Zn and Si as expected, but SIMS measurements also indicated a low level of unintentional impurities. Unintentional contaminants found at the epilayer–substrate interface and in the undoped layers included Si, C, and O. Si at the substrate interface is probably due to substrate surface contamination. A dip etch for 30 s in HF before growth reduced the C and O contamination to less than $1 \times 10^{16}\,cm^{-3}$ and reduced the epilayer–substrate interfacial Si by an order of magnitude to approximately $1 \times 10^{17}\,cm^{-3}$ with background carrier concentration levels in the undoped epilayer at less than $2 \times 10^{15}\,cm^{-3}$.

DLTS measurements were made on InP and GaInAs p–i–n diode structures. DLTS results, in conjunction with capacitance–voltage (CV) measurements indicated that the InP was n-type with a background carrier concentration at or below $5 \times 10^{14}\,cm^{-3}$. This is in general agreement with Hall measurements done on 6 μm thick InP samples which indicated 300 K carrier concentrations of $8.6 \times 10^{14}\,cm^{-3}$. DLTS measurements showed several traps in the band gap, but the total defect (trap) concentration was below $2 \times 10^{13}\,cm^{-3}$. Similarly, the GaInAs material was also shown to be of high quality with a similar background carrier concentration ($5 \times 10^{14}\,cm^{-3}$) as the InP, but with an even lower total trap concentrations of less than $1 \times 10^{11}\,cm^{-3}$. The dominant trap in the InP sample was located 0.47 eV below the conduction band with a concentration of $6 \times 10^{12}\,cm^{-3}$ [8]. This is consistent with literature values of a defect in InP related to phosphorus vacancies [9,10].

Two device performance metrics that are directly related to material quality and important from a device and systems perspective are DCR and after-pulsing. The DCR is the baseline performance metric that limits the amount of time a GM-APD can be biased above breakdown before a non-photon related avalanche event occurs. Modeling of the DCR combined with experimental data indicates that the dominate mechanism for 1.06-μm GM-APDs is trap assisted tunneling through the avalanche region via a defect that is approximately 0.34 eV below the conduction band [7]. This is in contrast to 1.55-μm GM-APDs where DCR is dominated by generation current in the small band gap absorber [7]. Comparing theory and experimental data we hypothesize that phosphorus vacancies (V_P) in the avalanche region are the most probable source of dark counts for 1.06-μm GM-APDs. The difference in the observed defect energy from DLTS and DCR experiments may be due to Frenkel–Poole barrier lowering caused by the high electric fields in the avalanche layer during DCR testing [11].

If V_P are the dominant mechanism for DCR, the device performance can be improved by limiting the number of V_P's formed during epitaxial growth. It has been reported that V_P's are dependent on growth conditions such as temperature and PH_3 overpressure [12,13]. Reducing the temperature or increasing the V/III ratio should reduce the V_P concentration [10]. Assuming that the formation energy for V_P is exponentially related to the temperature, a simple thermodynamic model can be constructed that suggests a 44% reduction in V_P concentration, and thus DCR, by reducing the temperature from 650 to 625 °C. Experimental data agree well with this simple model and a reduction in temperature yielded over 43% reduction in DCR, indicative that the V_P concentration was reduced by a similar amount. Fig. 2 shows the DCR density versus growth temperature. Further reducing the growth temperature to 600 °C did not show statistically valid improvement. Growth conditions, however, were not necessarily optimized as the V/III ratio in the vapor was kept the same as at higher growth temperatures. Since the phosphine cracking efficiency can be extremely temperature sensitive, it is reasonable to assume that the effective V/III ratio may be lower at 600 °C compared to 625 °C [14]. The decreased V/III ratio would increase the V_P concentration and help offset any reduction in V_P concentration from the lower temperature. This might explain the data observed from devices grown at 600 °C that show little to no change in DCR. Additional experiments will be conducted to further improve growth conditions at 600 °C in hopes of reducing the DCR.

All remaining experiments exploring the effect of growth rate and V/III ratio on DCR and after-pulsing were conducted at a growth temperature of 625 °C. Fig. 3 shows the effect of varying the V/III ratio on DCR density. Reduction in the V/III ratio to 55 showed approximately a three-fold increase in DCR density. It is expected that decreasing the V/III ratio should increase the V_P concentration, consistent with the hypothesis that V_P's are the likely source of dark counts in the device. Further experiments increased the V/III ratio to 220 and 330, respectively. The data do not show a significant decrease in DCR by increasing the V/III ratio above 110.

Growth rate may also affect inherent defects formed during OMVPE growth. Fig. 4 shows the results on DCR by changing the InP growth rate. The growth rate was

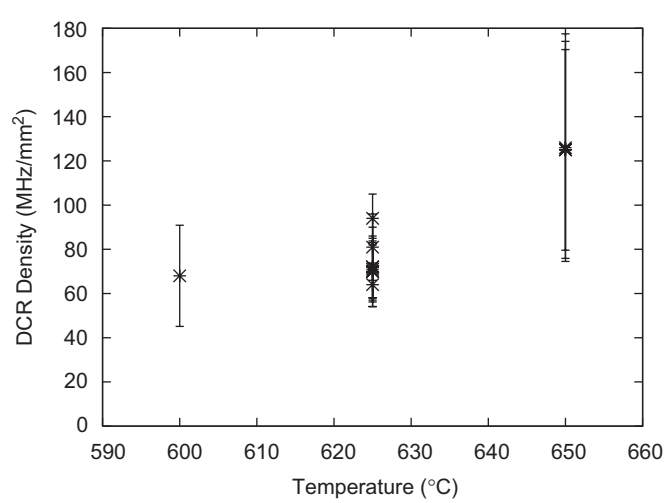

Fig. 2. DCR density versus temperature for GM-APDs. A 44% reduction in DCR density is seen by decreasing the temperature to 625 °C from 650 °C.

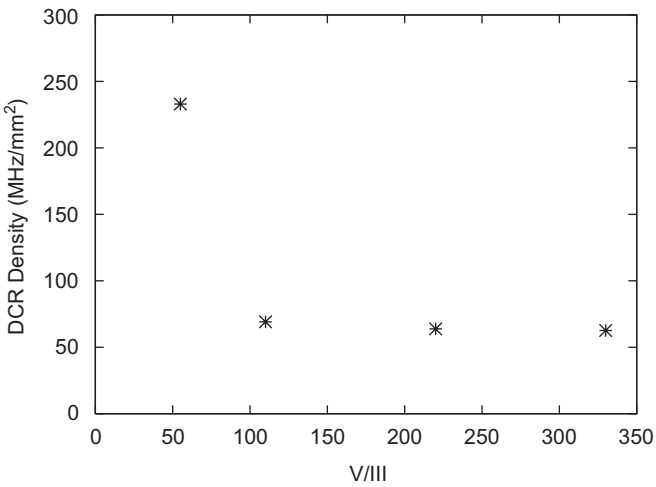

Fig. 3. DCR versus V/III ratio in the vapor. Increasing the V/III ratio from 55 to 110 decreases the DCR density significantly. Additional increases in V/III ratio show little to no decrease in DCR.

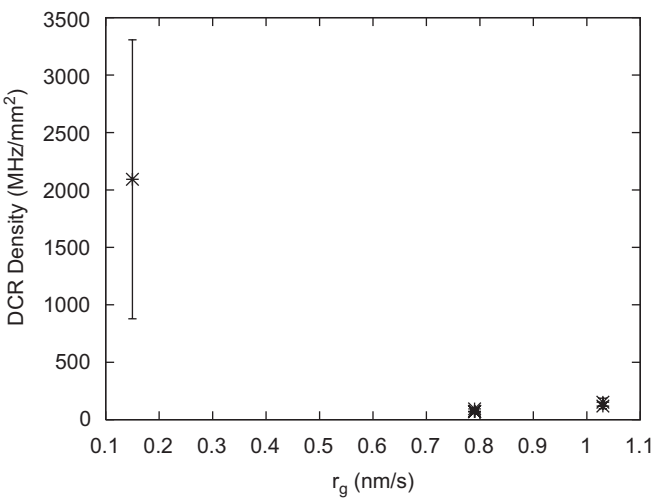

Fig. 4. DCR density versus InP growth rate. Growth rate in the InP multiplier region has a direct influence on DCR. Growth rate was chosen to give the best DCR performance.

decreased from 7.9 to 1.5 Å/s and then increased to 10.3 Å/s. CV measurements show a 2× increase in background carrier concentration for the lowest growth rate sample. However, this is unlikely to completely account for the 30× increase in DCR. Another potential issue with slower growth rate is enhanced Zn diffusion from the p-contact layer to the multiplier region. Zn is known to form a complex with P that increases V_P concentration [15,16] which would also increase the DCR. While the mechanism for increased DCR at the lowest growth rate sample is not entirely known, the large increase in DCR coupled with the increased growth time points to higher growth rates for improved APD performance. Data from the faster growth rate were slightly higher than the average result from our standard growth rate, but is in need of further investigation to determine if the slight increase is statistically significant or not.

In addition to dark counts, after-pulsing was also measured to determine the dead time of the APD. Dead time is the amount of time after an avalanche event that the GM-APD must be held below the breakdown voltage before being rearmed (biased above breakdown). During this dead time, the APD is not sensitive to photons. Thus, the dead time should be the minimum needed to ensure trap depopulation. If the number of traps can be reduced, the dead time should decrease. There is no correlation between after-pulsing and DCR results, so it is postulated that V_P's are not the primary mechanism for after-pulsing. However, experiments to date have been unsuccessful in identifying the exact nature of the defect.

Fig. 5 shows count rate versus hold off time for an after-pulsing measurement. Hold off time is the amount of time lapsed from the photon induced avalanche event. Measurements are complex and the data often require a multi-exponential fit, indicative that more than one trap is contributing to after-pulsing. Efforts to identify the dominant trap have been unsuccessful. Experimental data to date, suggests that the dominant trap causing after-pulsing is 0.1–0.2 eV from either the conduction or valence band. This energy is close to the unidentified 0.20 eV trap seen in DLTS experiments. Despite the similarity in energy level, further experiments are required to correlate the trap measured in DLTS and after-pulsing behavior. Even though the DCR has been reduced by improving growth conditions, after-pulsing has not been affected by any of the changes made in growth conditions. Table 1shows the number of filled traps/charge (N_{ft}/q) extrapolated from after-pulsing measurements for different growth conditions. No statistically significant change in N_{ft}/q is seen for the different growth conditions.

After-pulsing measurements done on "dummy" InP APDs as well as on 1.06- and 1.55-μm APDs also show no difference in after-pulsing behavior. This indicates that

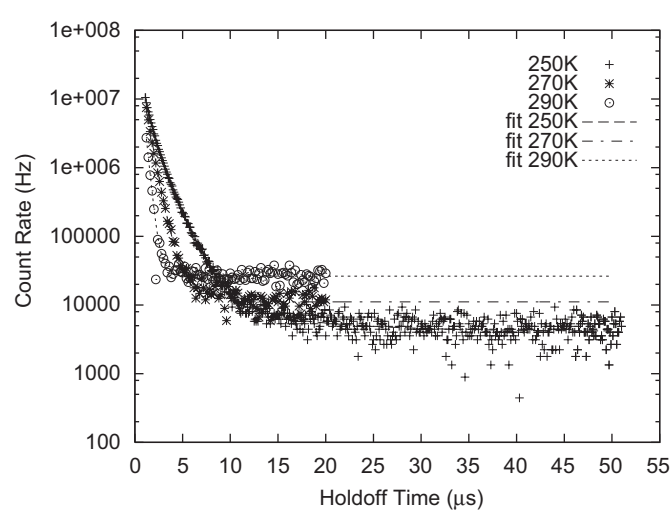

Fig. 5. Count rate versus hold off time (time since laser-induced avalanche) and exponential fits (lines) to data. Data are modeled using three exponentials indicative of multiple traps in the band gap contributing to after-pulsing events.

Table 1
After-pulsing results for various growth runs with different growth conditions. Despite changes in growth conditions, no change is seen in after-pulsing behavior indicated by the number of filled traps per charge (N_{ft}/q)

Run	T_g (°C)	V/III	r_g (Å/s)	N_{ft}/q
A	650	110	7.9	24
B	625	110	7.9	16
C	600	110	7.9	44
D	625	55	7.9	12
E	625	220	7.9	36
F	625	330	7.9	18

the trap responsible for after-pulsing is from something common to all three devices. This includes the InP avalanche and the Zn-doped contact layers. Changes in growth conditions discussed in this paper focused on the avalanche region and would not directly influence defect formation in other layers. In fact, experiments were designed to keep all other layers in the GM-APD the same during the varied growth experiments. Currently, experiments are being devised to explore the effect of Zn doping on after-pulsing in an effort to identify the dominant trap and whether it is bulk or interface related. Once identified, appropriate growth conditions will be examined in an effort to reduce the trap concentration and improve the dead time.

4. Summary

In summary, OMVPE growth conditions were investigated to improve the DCR and after-pulsing behavior of GM-APDs. Changes in the V/III ratio, growth temperature, and growth rate all affected the DCR of GM-APDs. The best performing GM-APDs are currently grown using a V/III ratio of 110, growth temperature of 625 °C, and a growth rate of 7.9 Å/s for InP. These growth conditions have lead to a 44% reduction in DCR compared to previously grown GM-APDs. However, after-pulsing measurements show no change despite the significant reduction in DCR. This indicates that the defect responsible for after-pulsing is different from the defect causing dark counts. Experiments on GM-APDs with different absorber materials show no difference in after-pulsing behavior and point to a defect in the InP avalanche or Zn-doped contact layers. We continue to explore possible mechanisms to explain after-pulsing and improve the dead time of InP-based GM-APDs.

Acknowledgments

The authors appreciate the technical assistance of L.J. Mahoney, K.M. Molvar, F.J. O'Donnell, D.R. Calawa, and S. Barriga. We would also like to acknowledge Evans Analytic Group for SIMS measurements and 4GEN Research, LLC for DLTS measurements and analysis.

References

[1] J. Donnelly, K. McIntosh, D. Oakley, A. Napoleone, S. Groves, S. Vernon, L. Mahoney, K. Molvar, J. Mahan, J. Aversa, E. Duerr, Z. Liau, B. Aull, D. Shaver, in: Proceedings of SPIE—The International Society for Optical Engineering, vol. 5791, Orlanda, FL, United States, 2005, pp. 281–287.
[2] K. Jensen, P. Hopman, E. Duerr, E. Dauler, J. Donnelly, S. Groves, L. Mahoney, K. McIntosh, K. Molvar, A. Napoleone, D. Oakley, S. Verghese, C. Vineis, R. Younger, Appl. Phys. Lett. 88 (13) (2006) 133503.
[3] S. Cova, M. Ghioni, A. Lacaita, C. Samori, F. Zappa, Appl. Opt. 35 (12) (1996) 1956–1976.
[4] D. Boroson, A. Biswas, B. Edwards, in: Proceedings of the SPIE—The International Society for Optical Engineering, Vol. 5338, San Jose, CA, USA, 2004, pp. 16–28.
[5] B. Aull, A. Loomis, D. Young, R. Heinrichs, B. Felton, P. Daniels, D. Landers, Lincoln Lab. J. 13 (2) (2002) 335–350.
[6] S. Cova, A. Lacaita, G. Ripamonti, Electron Device Lett. 12 (12) (1991) 685–687.
[7] J. Donnelly, E. Duerr, K. McIntosh, E. Dauler, D. Oakley, S. Groves, C. Vineis, L. Mahoney, K. Molvar, P. Hopman, K. Jensen, G. Smith, S. Verghese, D. Shaver, IEEE J. Quantum Electron. 42 (8) (2006) 797–809.
[8] S. Verghese, J.P. Donnelly, E.K. Duerr, K.K. McIntosh, D.C. Chapman, C.J. Vineis, G.M. Smith, J.E. Funk, K.E. Jensen, P.I. Hopman, D.C. Shaver, B.F. Aull, J.C. Aversa, J.P. Frechette, J.B. Glettler, Z.B. Liau, J.M. Mahan, L.J. Mahoney, K.M. Molvar, F.J. O'Donnell, D.C. Oakley, E.J. Ouellette, M.J. Renzi, B.M. Tyrrell, IEEE J. Sel. Top. Quantum Electron. 13 (2007) 870–886.
[9] W. Anderson, K. Jiao, in: A. Katz (Ed.), Indium Phosphide and Related Materials: Processing, Technology, and Devices, Artech House, 1992, pp. 82–102.
[10] R. Virkkunen, A. Seitsonen, M. Puska, R. Nieminen, Mater. Sci. Forum 143-4 (pt 3) (1994) 1305–1310.
[11] C.-C. Yeh, T.P. Ma, N. Ramaswamy, N. Rocklein, D. Gealy, T. Graettinger, K. Min, Appl. Phys. Lett. 91 (11) (2007) 113521.
[12] R.W. Jansen, Phys. Rev. B 41 (11) (1990) 7666–7673.
[13] N. Yamamoto, K. Uwai, K. Takahei, J. Appl. Phys. 65 (8) (1989) 3072–3075.
[14] N. Buchan, C. Larsen, G. Stringfellow, J. Crystal Growth 92 (1988) 605.
[15] C. Castleton, S. Mirbt, Phys. Rev. B (Conden. Matt. Mater. Phys.) 68 (8) (2003) 85203.
[16] J. Mahony, P. Mascher, W. Puff, J. Appl. Phys. 80 (5) (1996) 2712–2719.